Publ. Astron. Soc. Japan (2018) 00(0), 1–4
doi: 10.1093/pasj/xxx000

Bracketing the Galactic mid-infrared effective extinction for the filters used by the MSX, AKARI, WISE, and GLIMPSE surveys.

Maria Messineo

[1]ASTROMAGIC freelancer, Potsdam, Germany

Received ⟨reception date⟩; Accepted ⟨acception date⟩

Abstract

Extra plots

Key words: Mid-infrared effective extinction, $<A>/A_{K_s}$ are calculated for the broad-band filters used in the MSX, AKARI, WISE, and GLIMPSE surveys. The stellar model of an M0 star is reddened with the extinction curve and convolved with the filter profile. The average attenuation for these broad-band filters is, therefore, calculated. Three extinction curves are used: (i) a parametric formula for the extinction curve of the *dense* Orion OMC-1 cloud with a silicate peak at 1 (Rosenthal et al. 2000); (ii) a modification of the above mentioned formula to include the 3-8 μm data-points obtained for the Galactic center by Fritz et al. (2011); (iii) the new extinction curve obtained with spectra of early-type stars located in *diffuse* medium (Gordon et al. 2021). These curves are likely to encompass the bulk of possible Galactic values. Therefore, it is possible to properly quantify the uncertainty of the mid infrared effective extinction values.

1 Introduction

Extinction is a great tool to measure distances and to characterise the nature of individual stars. At end on 90s, when 2MASS and DENIS surveys were released, large Galactic maps of interstellar extinction become possible (Alard 2001; Schultheis et al. 1999, e.g.,). At near-infrared wavelength the extinction curve is usually approximated with a power law with an index, α: $A_\lambda \propto \lambda^{-\alpha}$. At that time, the near-infrared extinction law was approximated with a power law with index $\alpha = 1.61$ (Rieke & Lebofsky 1985). In the last two decades, the large amount of data allowed for a revision of the Galactic extinction curve, and, nowadays, an index α from 1.9 to 2.2 is usually assumed. In Messineo et al. (2005), by analyzing the 2MASS colors of late-type stars in the inner Galaxy a model with $\alpha = 1.9$ was preferred. From 2006 to 2011, several works reported α measurements from stellar colour larger than 2.0 (e.g. Nishiyama et al. 2006; Stead & Hoare 2009). Recently, Nogueras-Lara et al. (2020) reported a value of 2.2-2.4 by using stars in the nuclear Disk.

Fritz et al. (2011) observed Hydrogen lines at the Galactic Center and from their ratios derived $\alpha = 2.1$, in agreement with the stellar works.

When calculating the stellar luminosity, a set of extinction ratios is assumed and often uncertainties are neglected. These ratios may have an enormous impact on the derived luminosity. For example, as discussed in Messineo et al. (2005), for late-type stars at the Galactic center which suffer of about 2 mag of reddening in band H-K_s, the change of index from $\alpha = 1.61$ to $\alpha = 1.9$ implied a dimming of bolometric magnitudes of about 0.7 mag. A change of index from $\alpha = 1.9$ to $\alpha = 2.1$ implied another dimming of about 0.35 mag. An higher α makes the stars fainter. In Messineo et al. (2005), for the DENIS and 2MASS filters near-infrared effective extinction ratios $\langle A \rangle / A_V \propto \lambda^{-\alpha}$ were already presented for several α values, ranging from 1.61 to 2.2. As noted by Messineo et al. (2005), a different value of $R_V = A_V/E(B-V)$ does not affect $A_{K_s}/E(J-K_s)$ and $A_{K_s}/E(H-K_s)$, while the slope of the extinction curve does. The index α is an important parameter, as at near-infrared wavelength the same extinction law appear to be valid in any direction. At infrared light, extinction values can be inferred for individual objects anywhere, while at optical wavelengths, the local determination of the R_V parameter is

necessary.

Uncertainty in the mid-infrared extinction curve have only a secondary effect on stellar luminosities, as most of their light is emitted at short wavelengths. However, these ratios are important when estimating mass-loss, classifying stars on the basis of their stellar energy distribution and for determining envelope temperatures. The mid-infrared effective extinction ratios presented by Messineo et al. (2005) were partially based on approximations. There are newer determinations in literature. Mid-infrared effective extinction values have been measured with gas lines from the Galactic center region (Fritz et al. 2011), as well as with SPITZER spectra of early-type stars (Gordon et al. 2021). In the next section, these new results are implemented to obtain effective extinction values for the broad-band filters used by the MSX, GLIMPSE, WISE, and AKARI surveys.

2 Mid-infrared extinction power law

In Messineo et al. (2005), effective extinction values for the ISOGAL and MSX filters were calculated with three extinction curves; the extinction curve by Mathis (1990) which is based on a theoretic model; the parametric curve by Rosenthal et al. (2000) which was obtained in the OMC-1 cloud with H_2 observations; and a modified version of the latter to include the lack of the deep at 3-8 μm reported at the Galactic center with ISO spectroscopic observations by Lutz (1999). A constant value was adopted in the 3-8 μm region for Curve 3. The effective extinction values of Table 1 are obtained convolving the extinction curves with the M0 model by Fluks et al. (1994) and the filter response curves.

Two new extinction curves are here considered. Curve 4 is a modification of the Rosenthal fit, which replaces Curve3. The curve in the 3-8 μm region is modified with a linear fit to the H-line measurements at the Galactic center by Fritz et al. (2011). The linear fit is a decreasing function with increasing wavelengths. Curve 5 has been recently published by Gordon et al. (2021) and it is obtained with Spitzer spectroscopic data of early-type stars located in the direction of diffuse medium. The stars used by Gordon et al. are located at $A_V < 5$ mag. The Rosenthal analytic formula when used with a peak at 0.7 resembles that of Gordon et al..

At mid-infrared the extinction curve varies depending on the line-of-sight and on the type of medium in the path-way of the stellar light. The density of silicate dust is not an constant parameter. The peak of the silicate feature around 8-9 μm is 1-1.3 at the Galactic center, but it is only 0.7 in the solar neighbouring stars observed by Spitzer. The two sets of effective extinction derived with these two curves can draw constrains on the uncertainties of the effective extinction ratios. If the stellar environment is unknown, the Gordon curve can be taken as a lower limit curve, while the Galactic center curve as an upper limit curve. This allows to define an uncertainty for the effective extinction values.

3 Comparison with effective extinction values from broad-band photometry

Effective extinction ratios for the WISE and GLIMPSE filters were calculated by Wang & Chen (2019) by using broad-band photometry of red clump stars, which are primary indicators of distances by having known luminosity and colors. To assert the validity of the calculation made in this work, which is based on gas spectral data and stellar spectral data, a comparison is made with the results of Wang & Chen (2019) from broad-band photometry of giant stars.

When making comparison, particular attention to the normalisation factor must be paied. The effective extinction values $\langle A \rangle / A_{K_s}$ calculated in Table 1 for Curve 4 can be converted to $\langle A \rangle / A_V$ using a factor of 0.077, which is appropriated for an infrared power law of index $\alpha = 2.1$ and $R_V = 3.1$ (Messineo et al. 2005). This conversion factor is close to that (0.078) obtained by Wang & Chen (2019); for the curve by Gordon a conversion factor of 0.118 is calculated. Therefore, to locally explore the 2-20 μm region, it is preferable to re-normalize to K_s band. When re-normalizing the values to K_s-band, the agreement between the Wang's values and those from Curve 5 (Gordon et al. 2021) is good, though Gordon's curve gives smaller values for the WISE W3 and Spitzer [8.0] filters (the two filters that cover the 10 μm feature). The GLIMPSE [5.8] filter is particularly important because is not affected by the 10μm feature and is located in the 3-8 μm uncertain region of the Galactic extinction curve. While the stellar photometry of red clump stars yields $\langle A \rangle_{[5.8]} / A_{K_s} = 0.24$, and is consistent with the result from the SPITZER spectra (Gordon et al. 2021), the calculation based on the galactic center gas datapoints by Fritz et al. (2011) (CURVE 4) yields a larger value 0.38, and the calculation with the Rosental's curve of OMC-1 (CURVE 2) a value of 0.20. The depth of the extinction curve in the 3-8 μm region seems to be confirmed by clump stars, as well as by Spitzer spectra of nearby early-type stars. The 3-8 μm plateau observed with gas lines by Fritz et al. (2011) may be a peculiar feature of the Galactic center.

References

Alard, C. 2001, A&A, 379, L44

Fluks, M. A., Plez, B., The, P. S., et al. 1994, A&AS, 105, 311

Fritz, T. K., Gillessen, S., Dodds-Eden, K., et al. 2011, ApJ, 737, 73

Gordon, K. D., Misselt, K. A., Bouwman, J., et al. 2021, arXiv e-prints, arXiv:2105.05087

Lutz, D. 1999, in ESA Special Publication, Vol. 427, The Universe as Seen by ISO, ed. P. Cox & M. Kessler, 623

Table 1. Effective extinction, $\langle A \rangle / A_{K_S}$, using M-giant spectra (Fluks et al. 1994) for different bands defined by the ISOCAM and MSX filters (see Fig. 1).

Filter	$\lambda_{\rm ref}$	$\Delta\lambda$	Curve 1 (Mathis) ($A_{9.7}/A_{2.12} = 0.54$)	Curve 2 (Ros) ($A_{9.7}/A_{2.12} = 1.00$)	Curve 3 (Ros) ($A_{9.7}/A_{2.12} = 1.00$)	Curve 4 (Ros+Fritz) ($A_{9.7}/A_{2.12} = 1.00$)	Curve 5 (Gordon)	ave(Curve4, Curve5)
	μm	μm	$\langle A \rangle / A_{K_S}$	$\langle A \rangle / A_{K_S}$	$\langle A \rangle / A_{K_S}$	$\langle A \rangle / A_{K_S}$	$\langle A \rangle / A_{K_S}$	$\langle A \rangle / A_{K_S}$
ISO LW2	6.7	3.5	0.21	0.21	0.41	0.36	0.24	0.30 ± 0.06
ISO LW5	6.8	0.5	0.18	0.15	0.41	0.34	0.21	0.28 ± 0.07
ISO LW6	7.7	1.5	0.21	0.26	0.43	0.37	0.24	0.31 ± 0.07
ISO LW3	14.3	6.0	0.18	0.34	0.34	0.34	0.25	0.30 ± 0.05
ISO LW9	14.9	2.0	0.14	0.29	0.29	0.29	0.22	0.25 ± 0.03
MSX A	8.28	4.0	0.26	0.38	0.55	0.50	0.32	0.41 ± 0.09
MSX C	12.1	2.1	0.25	0.49	0.49	0.49	0.32	0.41 ± 0.09
MSX D	14.6	2.4	0.14	0.29	0.29	0.29	0.22	0.25 ± 0.03
MSX E	21.3	6.9	0.17	0.41	0.41	0.41	0.30	0.36 ± 0.05
Glimpse [3.6]			0.43	0.44	0.45	0.45	0.49	0.47 ± 0.02
Glimpse [4.5]			0.28	0.29	0.41	0.40	0.35	0.38 ± 0.03
Glimpse [5.8]			0.21	0.20	0.41	0.38	0.25	0.31 ± 0.06
Glimpse [8.0]			0.22	0.29	0.47	0.42	0.26	0.34 ± 0.08
WISE W1			0.49	0.48	0.49	0.49	0.53	0.51 ± 0.02
WISE W2			0.27	0.28	0.41	0.40	0.33	0.37 ± 0.03
WISE W3			0.28	0.53	0.55	0.55	0.36	0.46 ± 0.09
WISE W4			0.16	0.39	0.39	0.39	0.29	0.34 ± 0.05
AKARI S9W			0.28	0.42	0.57	0.52	0.33	0.43 ± 0.09
AKARI S18W			0.16	0.36	0.36	0.36	0.26	0.31 ± 0.05
Spitzer mips24			0.14	0.36	0.36	0.36	0.28	0.32 ± 0.04

Table 2. The $\langle A \rangle / A_V$ and $\langle A \rangle / A_{K_S}$ ratios of Wang & Chen (2019) for the WISE and GLIMPSE filters.

Filter	$\langle A \rangle / A_V$ Wang & Chen (2019)	$\langle A \rangle / A_V$ CURVE 4	$\langle A \rangle / A_V$ CURVE 5	
2MASS K_s	0.078 ± 0.004	0.077	0.118	
WISE W1	0.039 ± 0.004	0.038	0.063	
WISE W2	0.026 ± 0.004	0.031	0.039	
WISE W3	0.040 ± 0.009	0.042	0.042	
Spitzer [3.6]	0.037 ± 0.003	0.035	0.058	
Spitzer [4.5]	0.026 ± 0.003	0.031	0.041	
Spitzer [5.8]	0.019 ± 0.003	0.029	0.029	
Spitzer [8.0]	0.025 ± 0.003	0.032	0.031	
Filter	$\langle A \rangle / A_{Ks}$ Wang & Chen (2019)	$\langle A \rangle / A_{Ks}$ CURVE 2	$\langle A \rangle / A_{Ks}$ CURVE 4	$\langle A \rangle / A_{Ks}$ CURVE 5
2MASS K_s	1	1	1	1
WISE W1	0.50 ± 0.05	0.48	0.49	0.53
WISE W2	0.33 ± 0.05	0.28	0.40	0.33
WISE W3	0.51 ± 0.12	0.53	0.55	0.36
Spitzer [3.6]	0.47 ± 0.04	0.44	0.45	0.49
Spitzer [4.5]	0.33 ± 0.04	0.29	0.40	0.35
Spitzer [5.8]	0.24 ± 0.04	0.20	0.38	0.25
Spitzer [8.0]	0.32 ± 0.04	0.29	0.42	0.26

Mathis, J. S. 1990, ARA&A, 28, 37
Messineo, M., Habing, H. J., Menten, K. M., et al. 2005, A&A, 435, 575
Nishiyama, S., Nagata, T., Kusakabe, N., et al. 2006, ApJ, 638, 839
Nogueras-Lara, F., Schödel, R., Neumayer, N., et al. 2020, A&A, 641, A141
Rieke, G. H. & Lebofsky, M. J. 1985, ApJ, 288, 618
Rosenthal, D., Bertoldi, F., & Drapatz, S. 2000, A&A, 356, 705
Schultheis, M., Ganesh, S., Simon, G., et al. 1999, A&A, 349, L69
Stead, J. J. & Hoare, M. G. 2009, MNRAS, 400, 731
Wang, S. & Chen, X. 2019, ApJ, 877, 116

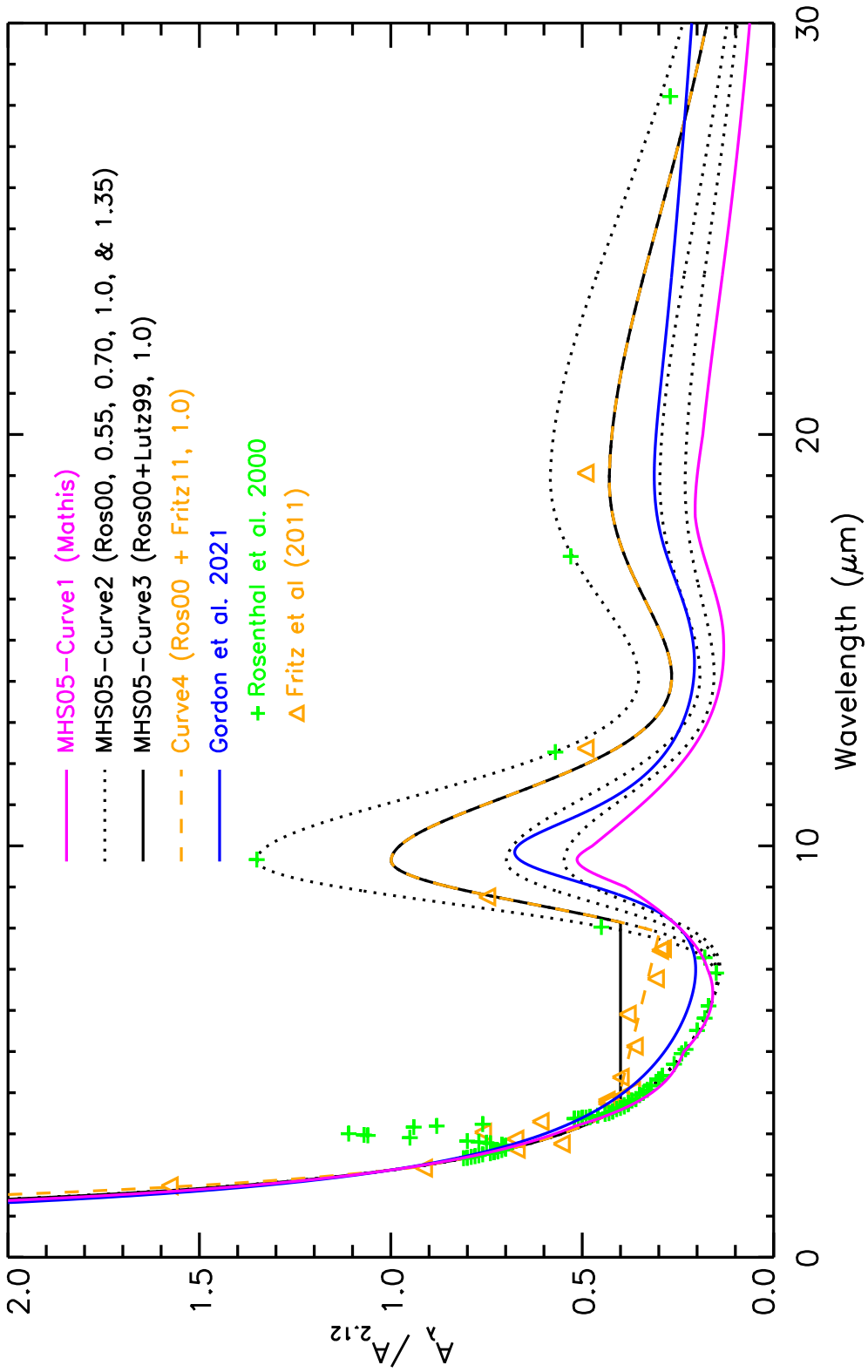

Fig. 1. Extinction curves as function of wavelength. The black dotted-dashed curve shows the parametric expression obtained by Rosenthal et al. (2000) in the Orion nebulae; a value of the silicate peak $A_{9.7}/A_{2.12} = 1.0$ (MHS05-Curve 2) is used. The curve is also shown without the minimum around 4-8 μm (MHS05-Curve 3, black continuous curve), as in Messineo et al. (2005), following Lutz (1999). The red continuous shows the Rosenthal's curve modified in the region from 3 to 8 μm using the more recent $A_\lambda/A_{2.12}$ values from H lines at the Galactic center by Fritz et al. (2011) (orange triangles) and adopting $\alpha = -2.1$ in the near-infrared. For comparison, the values from H_2 by Rosenthal et al. (2000) are indicated with green crosses. The blue curve is the recently obtained by Gordon et al. (2021) from diffuse medium.